

# Seismicity and Fluid Flow of the TAG Hydrothermal Mound -4:

Cruise Report

STAG Leg 4

R/V Knorr 180-1

October 24 – November 9, 2004

JASON2 Dive Program for Instrument Recovery

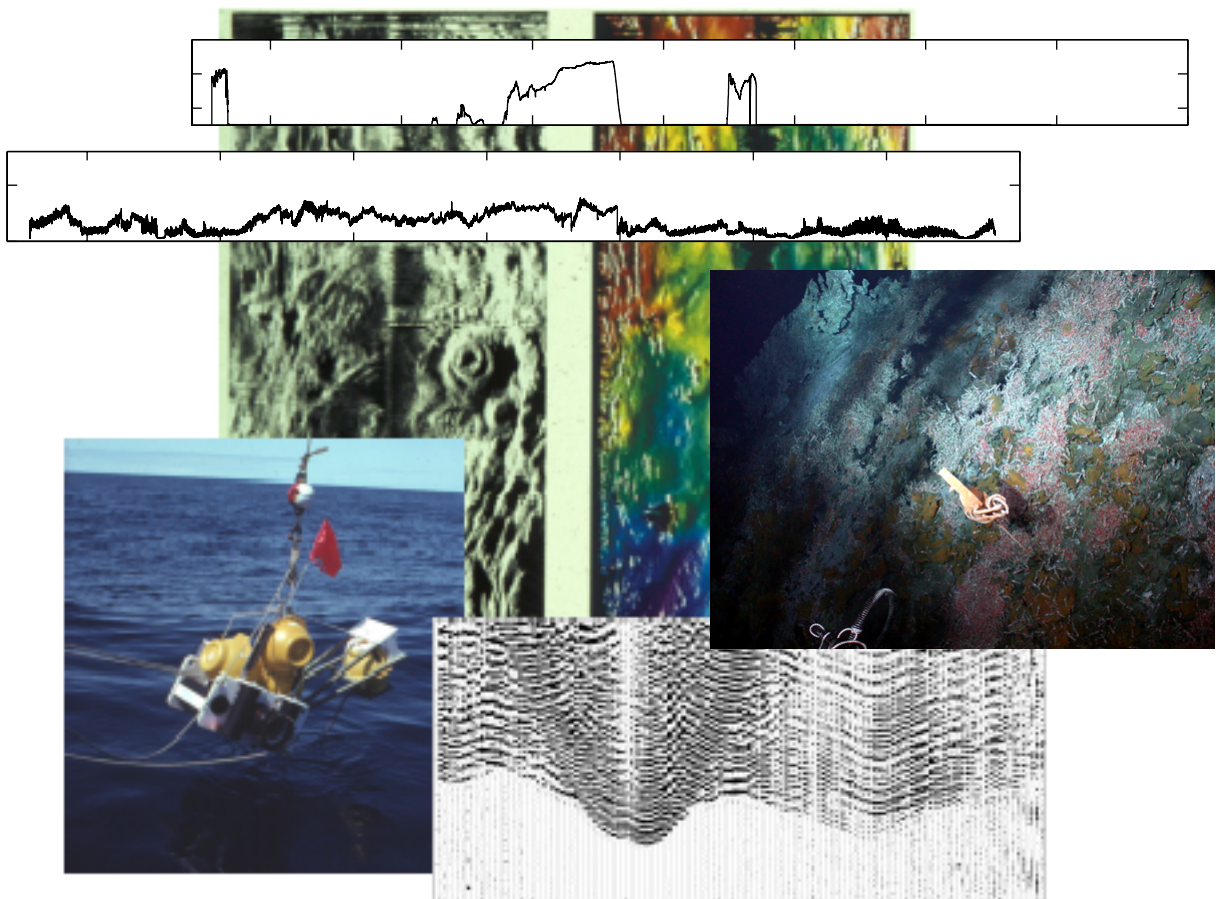


## Table of Contents

<b>1. Introduction</b>	p. 3-4.
<b>2. Cruise Objectives</b>	p. 4.
<b>3. Temperature Probes</b>	p. 4-7.
<b>4. Tide Gauge</b>	p. 7-8.
<b>5. Geological Samples</b>	p. 8-9.
<b>6. Biological Samples</b>	p. 10-14.
<b>7. Vent Fluid Samples</b>	p. 14-15.
<b>8. Water Column Plume Surveys</b>	p. 15-19.
<b>9. SM2000 Microbathymetry Survey</b>	p. 19-22.
<b>10. Green Laser Testing</b>	p. 22-23.
<b>11. Appendices</b>	
- A. Cruise Participants	p. 24.
- B. T-probe digital images	p. 25-31.
- C. Station Table	p. 32.
- D. Biological Specimen Lists	p. 33-34.
- E. JASON2 Navigation data	p. 35-36.

STAG Leg 4: Chief Scientist: Robert Reves-Sohn  
Co-Chief Scientist: Susan Humphris

# 1. Introduction

The TAG (Trans-Atlantic Geotraverse) hydrothermal field (26°08'N on the slow-spreading Mid-Atlantic Ridge) is one of the largest and best-studied sites of high-temperature hydrothermal activity and mineralization that has been found to date on the seafloor. Since the discovery of low-temperature hydrothermal activity and mineralization during the NOAA Trans-Atlantic Geotraverse (TAG) project in 1972–1973, the TAG hydrothermal field has been the subject of numerous investigations. International and multidisciplinary studies have included segment-scale multibeam bathymetry and geophysical studies; ship and submersible investigations of the active high-temperature sulfide mound; investigation of the relict hydrothermal zones within the field; monitoring of the active mound before, during and after drilling; and an ODP site survey with the DSL-120 side-scan sonar and Argo imaging systems of the rift valley and the high temperature active mound. In 1994, ODP Leg 158 drilled 17 holes ranging in penetration depth up to 125 m at the TAG active mound. All of these studies have resulted in a detailed understanding of the processes and physicochemical conditions that resulted in the formation of the TAG active mound and the underlying shallow stockwork, and have provided new insights into how large mineral deposits are constructed.

In spite of the aforementioned studies, several key aspects of hydrothermal convection at TAG are not understood. For example, the nature and location of the heat source that drives this large hydrothermal system remains a subject of speculation, as does the geometry of subsurface fluid flow. It is difficult to constrain these types of deeper subsurface issues with direct observations, but we have designed an experiment that will allow us to accomplish this goal by making simultaneous, long-term observations of vent-field microearthquakes, exit fluid temperatures, and tidal pressures. We will also use seismic refraction to estimate the crustal structure, including the possible presence of melts, along the length of the TAG segment. Our specific objectives are to:

- **Determine the location of the heat source and reaction zone for the TAG active mound**

There are two current models for deep hydrothermal circulation at the TAG active mound -- one of which invokes a heat source at the axial neovolcanic zone, and the other that predicts a heat source directly beneath the mound. We expect to be able to discern between these two possibilities in two complementary ways. First, an active source (airgun) seismic survey will provide evidence of any low velocity zones beneath the neovolcanic zone and/or in the vicinity of the TAG active mound that might represent the heat source location. Second, microearthquakes will delineate the depth of the brittle/plastic rheological transition, which specifies the maximum depth of fluid penetration into the crust, and possibly the location of the high-temperature reaction zone (where seawater is transformed into hydrothermal fluid).

- **Investigate the linkages and correlation between fluid flow, seismic activity, and tidal pressures to understand the hydraulics of the TAG active mound**

What determines the location and vigor of venting and mineral deposition in the TAG region? There is strong evidence from the TAG active mound and from volcanic-hosted ore deposits in ophiolites that faulting plays a key role in maintaining fluid-flow pathways, and a direct correlation between fluid flow and local seismic activity has recently been demonstrated in modern deep-sea systems [*Johnson et al.*, 2000; *Sohn et al.*, 1998]. In addition, changes in the flow within the shallow subsurface at

the TAG active mound are manifest at its surface by changes in its morphology and in the distribution of venting on very short time scales. We will quantify the spatial and temporal patterns of microearthquake activity in the TAG region, and correlate them with temperature time series data from high- and low-temperature orifices on the TAG mound. We will also investigate any correlation between exit fluid temperatures and/or seismic activity with the tidal signal. These analyses will provide a first-order view of the hydraulics at TAG.

## 2. Cruise Objectives

This cruise is the final leg in a sequence of four expeditions. The first expedition was conducted from June 21 – July 8, 2003 on the *R/V Atlantis*, with the principal objective of deploying the ocean bottom seismometer (OBS) and temperature probe networks on and around the TAG mound. The second expedition was conducted from October 24 – November 9, 2003 on the *R/V Maurice Ewing*, with the principal objective of shooting a seismic refraction survey on the TAG segment. The third expedition was conducted from March 16 – April 10, 2004 on the *R/V Knorr*, with the principal objective of recovering the OBS network. The fourth leg (this cruise) consisted of two dives with the JASON2 ROV. The first dive (108) was dedicated to temperature probe recovery, microbathymetric mapping, and sampling on the TAG mound. The second dive (109) was dedicated to water column plume surveying, microbathymetric mapping, a geologic survey of the eastern valley wall, and sampling.

The primary objectives of this cruise were to;

- 1. Recover temperature probes on the TAG mound.**
- 2. Recover a deep-sea tide gauge located ~400 m NW of the TAG mound.**

Secondary cruise objectives were to;

- 1. Acquire micro-bathymetric data of the TAG mound.**
- 2. Acquire sulfide samples for geochemical and microbiological analyses.**
- 3. Map the TAG water column plume.**
- 4. Acquire biological samples of vent fauna.**
- 5. Acquire black smoker fluid samples and their associated sulfide deposits.**
- 6. Acquire sediment samples for meiofaunal and geochemical analyses.**
- 7. Conduct a visual reconnaissance of the eastern axial valley wall lithostratigraphy.**
- 8. Test a green laser system for water column plume detection.**

## 3. Temperature Probes

(Rob Reves-Sohn)

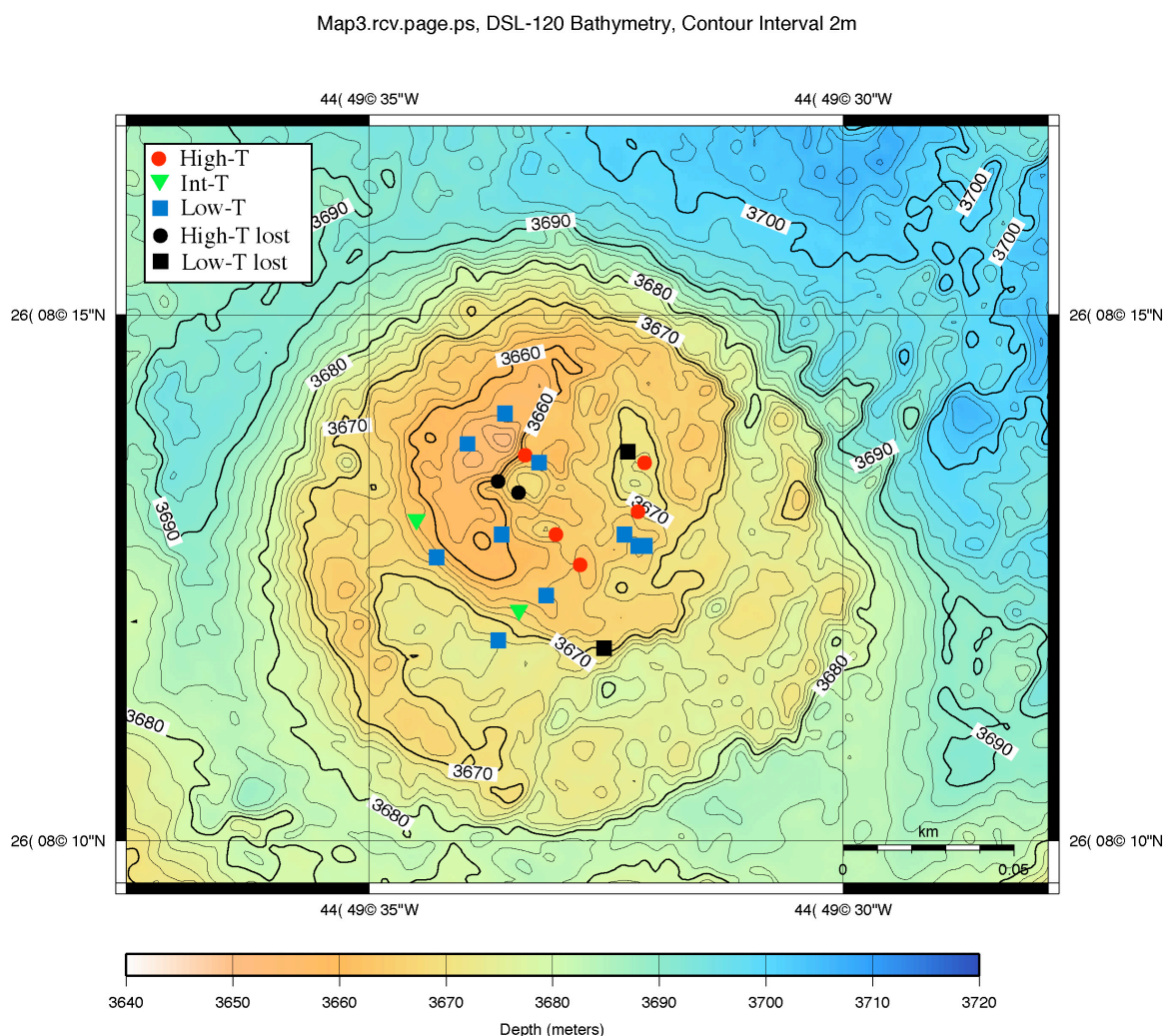
### 3.1 Probe recovery

Two basic types of temperature probes were deployed during STAG Leg 1 using the DSRV Alvin in June, 2003; (1) High (152 to 460°C) and Intermediate (-2 to



124°C) Temperature Probes designed by Deep Sea Power and Light (San Diego, CA), and (2) Low (-2 to 60 or 70°C) Temperature Probes designed by VEMCO Ltd., (Nova Scotia, Canada). For a more detailed description of these probes please see the cruise report from STAG Leg 1.

The high- and intermediate-temperature probes were deployed in black smoker orifices near the center of the mound, while the low-temperature probes were placed in diffusely venting cracks with shimmering water. Five of the seven high-temperature probes, both of the two intermediate-temperature probes, and all 12 of the low-temperature probes were recovered. High-temperature probes #1 and #7 were not found. The marker for probe #1 was located, but was found beneath a large sulfide block that had apparently fallen from the summit. The area near the marker was thoroughly searched, but the probe could not be located, in spite of the fact that extensive excavation was undertaken. Probe #7, the so-called Boomer probe, had no marker owing to the fact that it was hung over the side of a large vent orifice on a vertical cliff face. We found the Boomer vent, but the chimney structures around it had grown considerably since the deployment, and the entire area was covered in shrimp swarms. The chimney structures may well have grown over the probe during the deployment, but in any case we could not locate the probe. Locations of the recovered probes on the mound are shown in Figure 1.



The hydrothermal context of many of the probes changed during the course of the deployment. The black smoking orifices near the base of the central cone into which several of the high-temperature probes had been lanced were found to be inactive upon recovery. Several of the wands housing the low-temperature probes were knocked over, and two of the low-temperature sites were venting high-temperature fluids during recovery. High-resolution digital images of each probe prior to recovery can be found in Appendix B.

### 3.2 Temperature Probe Data

All of the recovered probes contained a full set of data except for low-temperature probes #3 and #10. These probes were subjected to temperatures in excess of their limits and were badly burned. Burn scars and high-temperature sulfide deposits are readily evident on the pressure housings and yellow wands of these two low-temperature probes, and upon opening the pressure housings a noxious blue smoke was released. This is most likely a result of an internal battery fire. Each low-temperature wand houses two probes that operated independently. Both probes functioned and returned nearly identical records for all wands except for probe #11. One of the probes on this wand had no data upon recovery, and it appears the probe never started. The cause of this failure is unknown, but operator error is a possibility. The other probe on the wand functioned normally, however, so no data was lost as a result of the failure. The high-temperature probes returned measurements every 10 minutes from 6/27/03 11:00 to 5/13/04 20:00 GMT. Intermediate-temperature probe #13 returned measurements every 4 hours from 6/28/03 17:56:07 to 04/23/04 13:56:07 GMT. Intermediate-temperature probe #14 returned measurements every hour from 06/29/03 12:00 to 05/25/04 11:00 GMT. Low-temperature probes returned measurements every 8 minutes from 06/27/03 11:00 to 06/24/04 19:56 GMT. Data records for the high- and intermediate-temperature probes are shown in Figure 2. Data records for the low-temperature probes are shown in Figure 3.

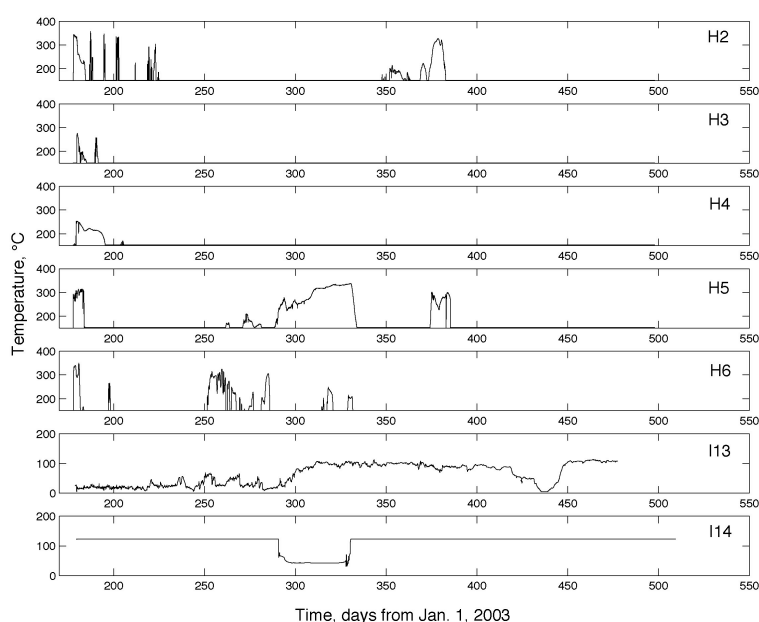


**Figure 2. High-temperature and intermediate-temperature probe data records.**

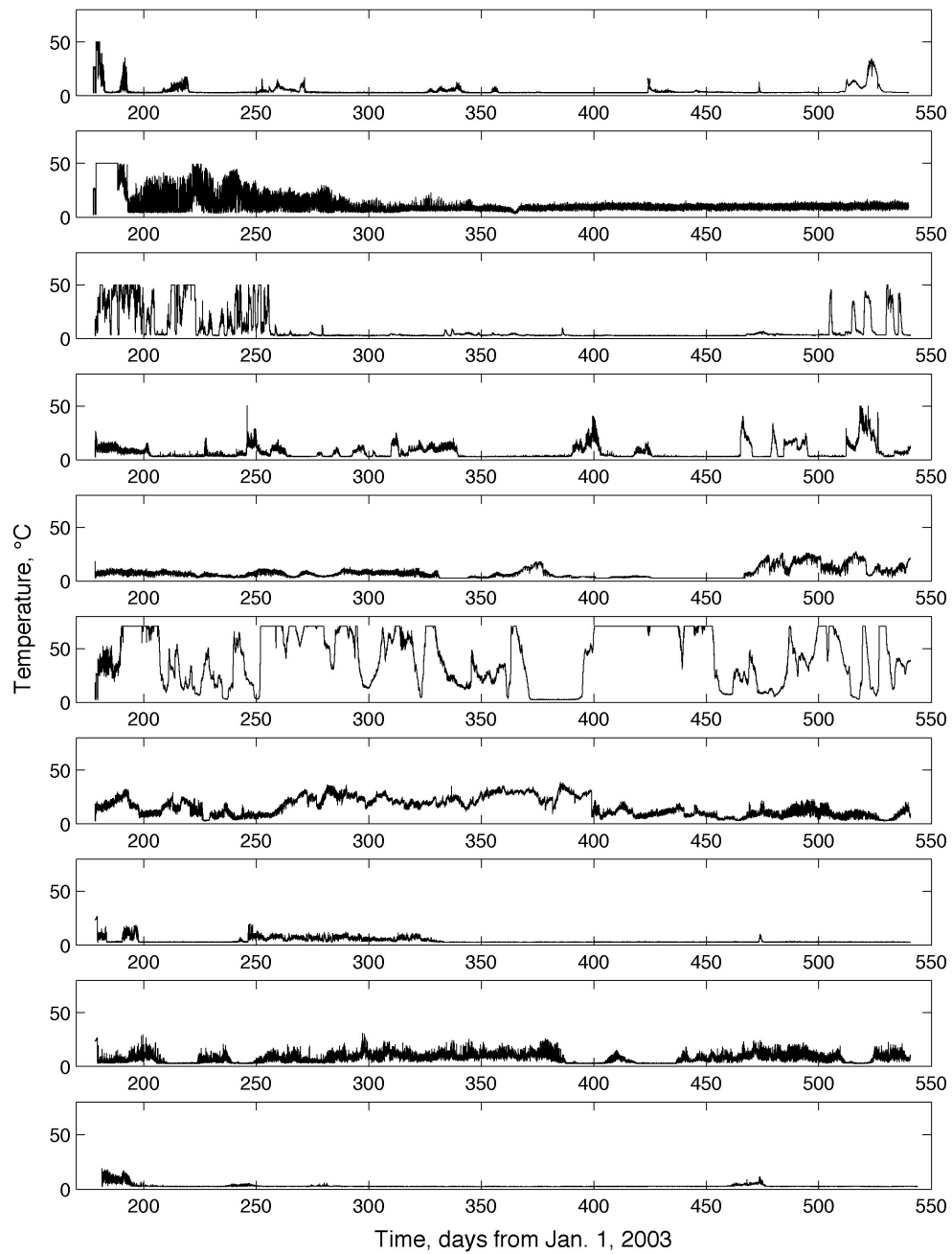


**Figure 3. Low-temperature probe data records.**

## 4. Tide Gauge

(Rob Reves-Sohn)

A SeaBird SBE26 Wave and Tide Gauge instrument had been deployed during STAG Leg 1 to measure tidal pressure signals during the experiment. The gauge was programmed to make tidal measurement every 10 minutes, providing 144 samples per

day, a memory endurance of 14478 days, and a battery endurance of about 3 years (based on the matlab script *tdgag\_pwr.m*). The tide gauge was recovered during the second dive. Upon recovery it was determined that the D-cell batteries had failed after ~6 months of recording. The tidal pressure and temperature measurements recorded by the tide gauge are shown in Figure 4.

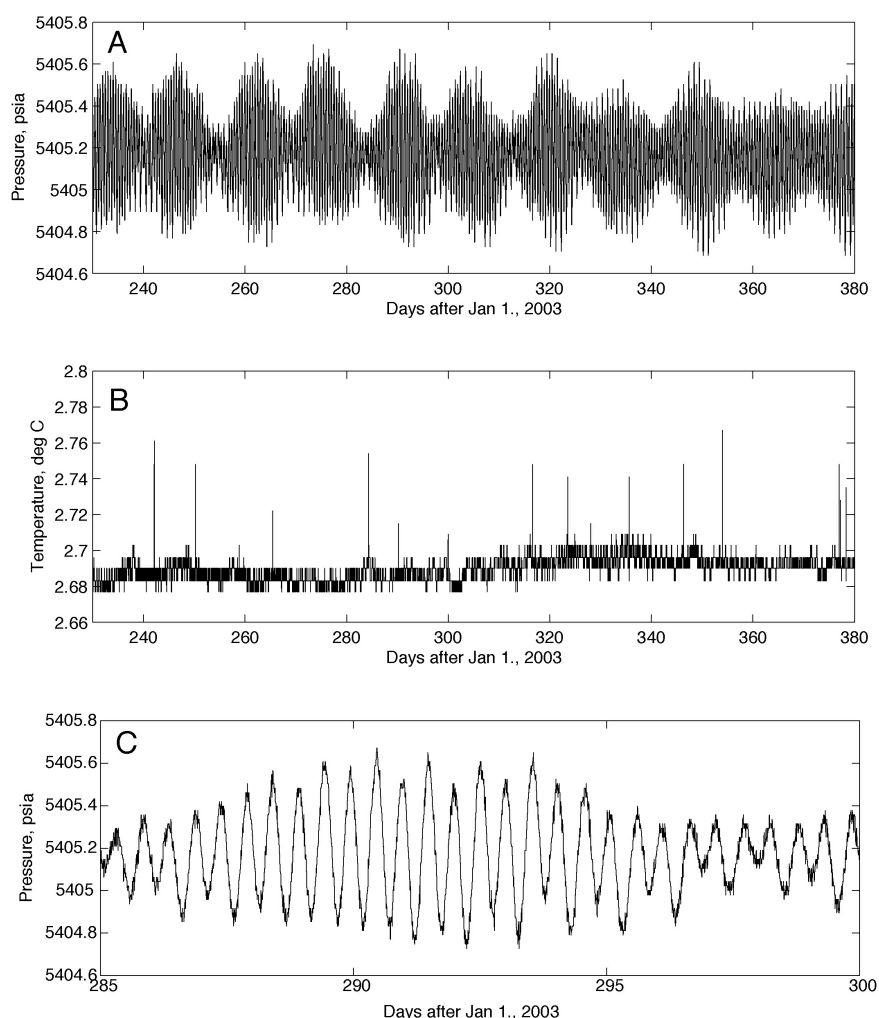


**Figure 4. Tide gauge data. (A) Pressure. (B) Temperature. (C) Two-week pressure record.**

## 5. Geological Samples

(Susan Humphris)

A series of sulfide samples were taken in a transect from south of the TAG mound to the black smoker complex to investigate the changes in microbiological activity with increasing distance from the area of high temperature hydrothermal discharge. Six samples were collected, ranging from sulfides almost completely weathered to Fe-oxhydroxides, to massive pyrite showing various stages of oxidation on the lower and upper platforms, to walls of an active (366°C) black smoker chimney (Figures 5-6). Sample descriptions and positions are provided in Appendix C. Sub-samples were frozen (-80°C) for shore-based microbiological analysis as part of the research of Dan Rogers, a WHOI-MIT Joint Program student in Marine Chemistry & Geochemistry.

The remainder of the samples were dried and stored for return to WHOI where they will be available for mineralogical and geochemical analyses.

In a survey of the lower portion of the rift valley wall to the E. of the TAG mound, a sample of gabbro was collected from a depth of 3082 m (Station J2-109-2).

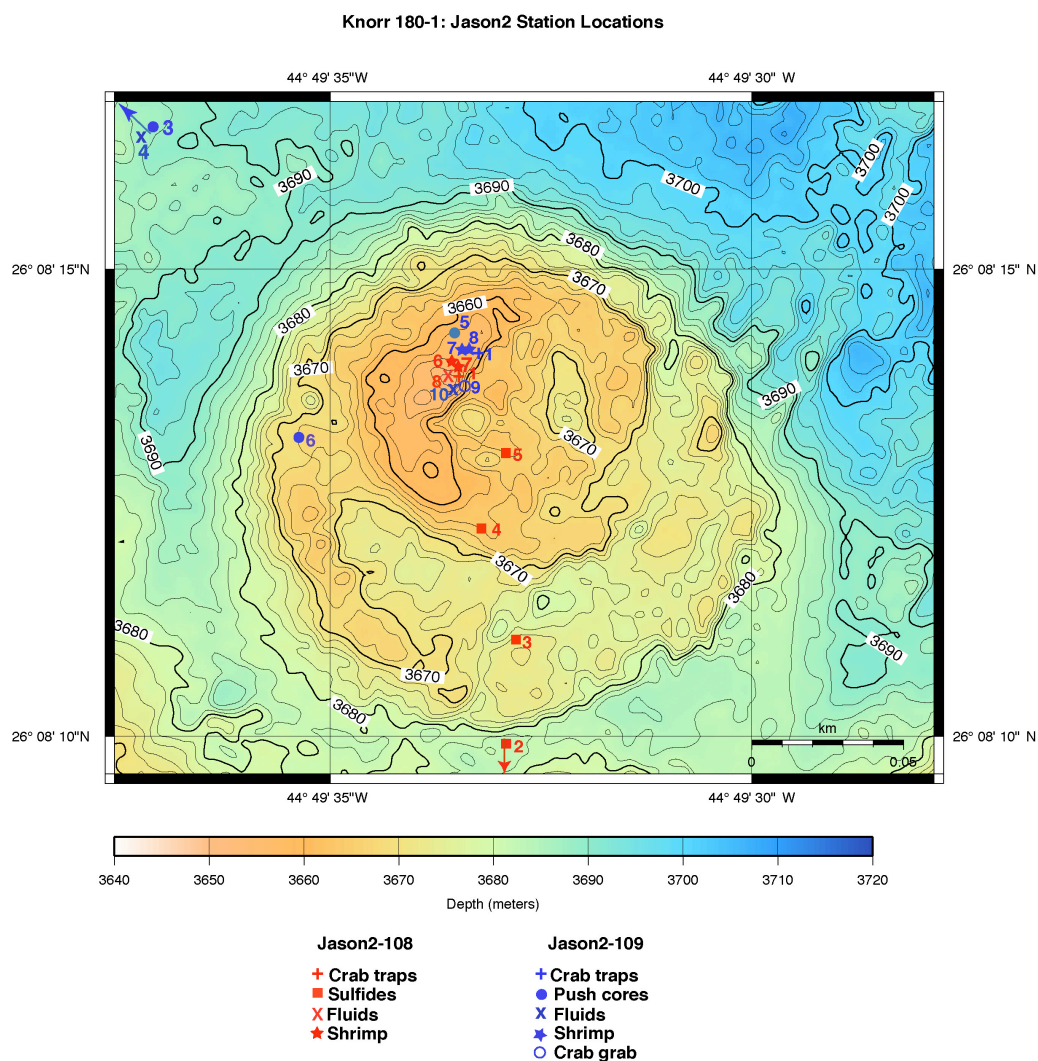


**Figure 5. Station location for biological, geological, and fluid samples.**



**Figure 6. Sulfide sample from active chimney.**



## 6. Biological Samples

(Rhian Waller, Jon Copley, Hannah Flint)

Biological collections were made on both Jason2 ROV dives using a double chamber hydraulic slurp, multiple crab traps and push cores. These collections were specific to either WHOI or SOC goals and are described below in more detail.

Dive J2-108 deployed two crab traps close to the ‘Boomer’ chimney. Only one trap was recovered during this dive, as prevailing tidal conditions prevented the retrieval of one of the traps that was placed under a ledge, with black smoke reducing visibility. The other crab trap was on top of a saddle beside ‘Boomer’, and so was retrieved from the other side of the smoker chimney. Slurp samples were then taken beneath the crab traps. During deployment of the slurp gun it was noticed that it did not have sufficient suction to retrieve adults, and this was confirmed by the predominance of juveniles within both chamber samples. The mesh size covering the slurp outlet was changed (to a coarser mesh) to attempt to remedy this problem.

Dive J2-109 first located the crab trap that was left behind. This trap had fallen down slope, and was left in this position throughout the dive. Two further crab traps were deployed just below the fallen crab trap, next to several small black smoker chimneys. Six push cores were attempted in various locations on this dive, and four successful cores were obtained. On retrieval of the three crab traps, two slurp samples were taken. Again, it became apparent that the slurp did not have sufficient suction to retrieve adult shrimp, which was confirmed on the surface. The slurps also retrieved fewer individuals than the previous dive. Two crabs located down slope from ‘Boomer’ were also grabbed with the manipulator and placed in the biobox.

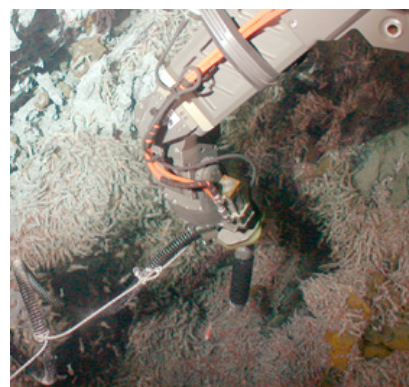


**Fig. 7 – Slurp sample being taken on dive J2-108**

### 6.1 WHOI Goals

The main objective of WHOI biological sampling during this cruise was to examine the spatial and temporal effects of a slow-spreading mid-ocean ridge on intraspecific phylogeography, patterns of dispersal, and rates of gene flow. The main species for this work is the shrimp *Rimicaris exoculata*, as well as other vent shrimp species.

Genealogical methods will be used alongside DNA-based data to provide robust estimates of gene flow and population parameters relevant to the dispersal and phylogeography of vent-endemic organisms.

The results will be added to those obtained from previous MAR and EPR cruises for

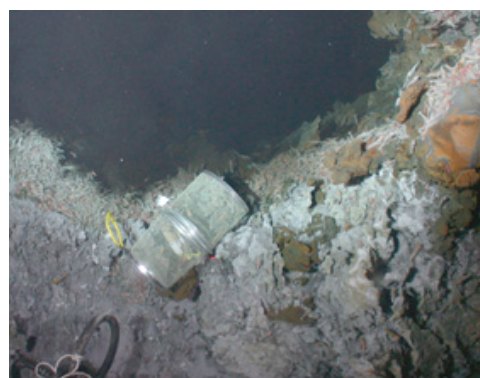


**Fig. 8 – Crab trap deployed on J2-108 in a saddle with Boomer to the right**

ongoing molecular genetic analysis. A secondary goal of this cruise was to collect shrimp, vent-associated fauna and sulphide samples for epibiont work by graduate student Abigail Knee. Shrimp epibionts will be investigated using Florescent InSitu Hybridization techniques (FISH) and compared to bacteria living on other species around the same vent site, to elucidate whether they are obligate to shrimp or more common around vents.

The sampling strategies employed involved deploying crab traps baited with tinned cat food and hydraulic slurping using ROV Jason2. Two crab traps were also placed on the elevator to be deployed off axis. These elevator crab traps did not collect any crabs, though 6 species of general deep-sea amphipod were collected and shall be added to our genetic database of deep-sea fauna. Two crab traps were deployed during J2-108, though only one retrieved. These traps were placed beside the 'Boomer' black smoker. The one crab trap retrieved did not contain any crabs, however did yield adult *Rimicaris exoculata*. Two areas were slurped around 'Boomer', one area with primarily adults and one area with primarily juveniles to investigate connectivity between adult and juvenile swarms usually found around these vents. Because of the slurp not having sufficient suction, both slurp samples

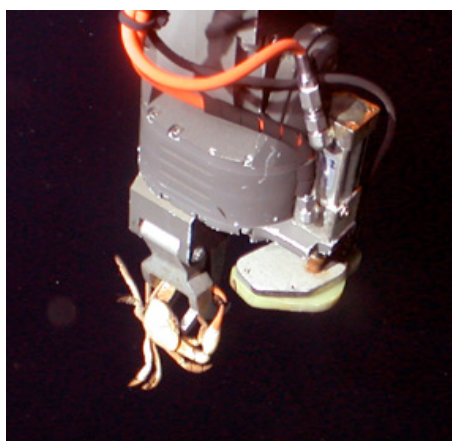


**Fig. 9 – Crab grabbed during J2-109**

contained only juvenile *R. exoculata*. From the video footage it is an interesting observation that in all areas around the 'Boomer' smoker, juvenile *R. exoculata* appeared to be living below the adult population, rather than in discrete colonies. Sulphides were collected by Susan Humphris (WHOI) and sub-samples were taken from three locations and preserved for epibiont work.

On dive J2-109 the crab trap not collected from the previous dive was located (and had fallen down slope) and two more crab traps were deployed. The fallen crab trap remained in its position until the end of the dive, as it appeared to be in a small black smoker area, with shrimp swarms and crabs. All three crab traps were retrieved, though only one contained a single crab, alongside adult *R. exoculata* and *Chorocaris chacei*. Because of the lack of crabs in the traps, it was then decided to grab two crabs with the manipulator and place them in the biobox. These were taken from just below 'Boomer'. Slurp samples of adult and juvenile populations were also taken beside the lower crab traps, though as before the sample was primarily juvenile *R. exoculata*.

Shrimp samples were measured to add to continuing population data, and 50 samples of adult and juvenile *R. exoculata* had DNA extracted from fresh tissue. Due to the paucity of adult *R. exoculata*, samples were split, with the head going to Jon Copley (SOC). Abdomens (or whole shrimp in the case of juveniles) were quickly frozen at -70°C to preserve DNA for later analysis (Appendix D, Table D1). Subsets of shrimp, crabs and sulphides taken for epibiont work were washed in filtered seawater prior to freezing at -70°C (Table D2). Amphipods from the elevator crab traps had a subset of specimens placed in 95% Ethanol for taxonomy, and the remaining individuals frozen at -70°C. All samples taken will be stored and analyzed in Tim Shank's laboratory, WHOI.

## 6.2 SOC Biology Goals

### 6.2.1 Reproductive biology of vent shrimp

Shrimp were collected for histological examination to assess any seasonality in their reproductive development. Previous samples from TAG suggest aseasonal reproduction but are limited to July - September. The paucity of ovigerous females in these samples, however, could be consistent with seasonal reproduction outside this sampling period. Seasonal reproduction is now known in the bresiliid shrimp *Alvinocaris stactophila* at a cold seep, for example, with females carrying eggs from November to February/March.

A two-chamber slurp gun was used to collect shrimp from dense aggregations within 1-2 metres of visible black smoker sources. On each ROV dive, the attempt was made to sample a patch dominated by adult shrimp into one chamber and a patch of juveniles into the other. All slurp gun samples, however, showed strong bias towards juvenile shrimp. This may have resulted from poor suction, which adults may have been able to evade with better swimming ability. The exhaust of the slurp gun chamber also appeared to clog rapidly on video, reducing suction further. These conditions persisted during both dives, despite increasing the mesh size of the exhaust to improve suction. Shrimp were also recovered, however, in crab traps deployed in the vicinity of the slurp gun samples.

The thoraxes of a total of 70 adult and 28 "adolescent" *Rimicaris exoculata* were collected to examine reproductive development (see summary Table below). "Adolescent" *R. exoculata* were distinguished from juveniles, often of similar length, by having dorsal photoreceptor organs and branchial carapace both similar in shape to adults. Total length and carapace length were measured for adult and adolescent specimens using vernier calipers. Males were identified by the asymmetrical mesial extension on the endopod of pleopod 1 seen under a dissecting microscope. This feature is not always clear in "adolescent" males, however, and some small males may be misidentified as females. Thoraxes were fixed in 10% buffered seawater formalin for 48h and subsequently preserved in 70% isopropanol. The thoraxes of five *Chorocaris chacei* were also preserved for descriptive comparison with *R. exoculata*. The corresponding abdomens of all specimens were allocated to the Shank molecular study. Histological processing and examination will take place at SOC.

Although confirmation will require the results of histological investigation, initial examination of visible ovarian development suggests that females exhibit considerable intrasample variation (ranging from no development to ripe ovaries), similar to previous samples from July - September. This pattern appears consistent with asynchronous (aseasonal) reproduction. All samples during this cruise were collected from dense aggregations of shrimp in the close proximity to high-temperature hydrothermal sources. No ovigerous females were recovered in samples; if reproduction is asynchronous, the location of ovigerous females at TAG remains unresolved.

### 6.2.2 Trimethylamine oxide content of deep-sea crustaceans

Vent shrimp were also collected for determination of the trimethylamine oxide (TMAO) content of their muscle tissue. Deep-sea crustaceans contain elevated levels of TMAO in their tissues as an adaptation for protein stabilisation under high pressure; concentrations of this osmolyte usually increase with habitat depth.



Previous work, however, shows that vent shrimp have lower levels of TMAO than expected for the depth at which they live, possibly as a result of its reduced effectiveness as a protein-folding chaperone at elevated temperatures.

At total of 161 juvenile and 35 "adolescent" *Rimicaris exoculata* were frozen whole at -70C to examine ontogenetic change in TMAO content in this species. Five abdominal muscle samples of *Chorocaris chacei* were also frozen to compare the TMAO content of this species (see summary Table D3). To provide a comparison with non-vent crustaceans from a similar depth, 10 non-vent amphipods (all provisionally identified as *Eurythenes*) were isolated and frozen from the bait in the crab traps deployed on the elevator. All analyses will be carried out at SOC.

### 6.2.3 Push Cores

Push core material was provided for three projects:

1. Abundance and species diversity of the meiofauna (organisms between 45µm and 0.5mm) in chemosynthetic environments of the deep-sea (Hannah Flint, SOC).
2. DNA, microbial populations, biomarkers and trace metal distribution across sharp redox boundaries associated with sulfidic sediments at TAG (Rachel Mills, SOC).
3. Material containing iron (hydr)oxides sediments from the non-buoyant hydrothermal plume was acquired for analysis of transition metal uptake. The proposed project aims to investigate the link between metal uptake into colloidal plume precipitates, via adsorption and incorporation, and oceanic bioavailability of biolimiting elements (Caroline Peacock, Univ. Bristol / SOC).

The push coring took place during the second JASON 2 dive on the 04 November 2004. Six cores of 6.5 cm diameter and 27cm length were secured in the basket.

**Table 5 – Push Core Sample Summary**

Core No.	Sediment Type	Station	Time (GMT)	Outcome	Project no. assigned to.
1	Sulfidic	1	00.29	Successful	1
2	Pelagic	3	17.35	Successful	3
3	Pelagic	3	17.39	Unsuccessful	-
4	Sulfidic	6	01.31	Successful	2
5	Sulfidic	5	00.50	Unsuccessful	-
6	Pelagic	3	17.49	Successful	1

Once JASON 2 was retrieved, push cores were loosened from the basket and taken individually into the lab. Here a bag was placed over the end of each holder and all cores were placed in the fridge.

**Core 6** was assigned for quantitative abundance and taxonomic meiofaunal work so processing had to ensure that every piece of material and drop of water in and associated with the core was passed through a 45µm mesh sieve. The majority of this core had dropped down into the holder and so a photo wasn't taken. The tide mark on the side of the core indicated a sediment height of 10.5cm. The sediment was extracted into a 45µm mesh sieve. The material in the sieve was then rinsed with

filtered sea water until the water running through ran clear. The sample was then preserved in 10% buffered formalin.

**Core 2** was processed for the transition metal uptake project. This core was photographed and measured to consist of 10.5cm length of sediment. This core was sliced into 1cm slices and preserved in bags in the 4°C fridge. As this core retained water, it was drained through the 45µm mesh sieve and preserved in gluteraldehyde for EM work by H. Flint (SOC).

**Core 4** was assigned chiefly to the proposed redox boundary project by R. Mills (SOC). The core material was extruded and sliced in half, one half being placed in a pot and submerged in filtered sea water for qualitative meiofaunal work. The other half was cut into 1cm intervals. These subsamples were placed in glass vials and sealed. Every fourth slice was cut in half and one half stored in glass vials under nitrogen and stored at 4°C in a nitrogen atmosphere.

All the other vials were frozen at -70°C. The meiofaunal sample was processed as per core 6 but the final rinse and preservation was with 95% ethanol to allow for molecular work.

**Core 1** was processed for quantitative meiofaunal abundance and taxonomic work and so was processed as per core 6 and washed into a pot with 10% buffered formalin. The majority of this core had dropped down into the holder. The mark left around the side of the core indicated a sediment height of 7cm.

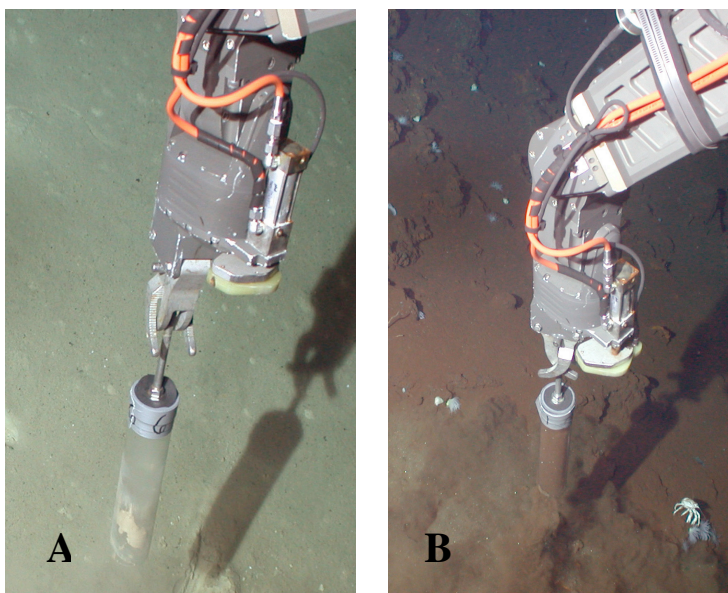


**Fig. 10 – A, Core 6 second attempt; B, Core 1 successfully taken**

## 7. Vent Fluid Samples

(Darryl Green)

Six high-temperature hydrothermal vent fluid samples and two background seawater samples were obtained using titanium major water samplers. Although it was not possible to obtain samples from the same orifices sampled during STAG Leg1, because one was no longer venting and the other was covered by a flange, the high-temperature samples were collected from the main active mound in close proximity to these sources. Four were obtained at station 8 during Jason II lowering #108 and a fluid temperature of 366°C was recorded (Figure 11). The other two and the background seawater samples were collected at stations 10 and 4, respectively, during lowering #109. Alkalinity, pH, [H<sub>2</sub>S], [Br<sup>-</sup>] and [SO<sub>4</sub>], were determined onboard. Further analyses will be undertaken at the Southampton Oceanography Centre, UK.

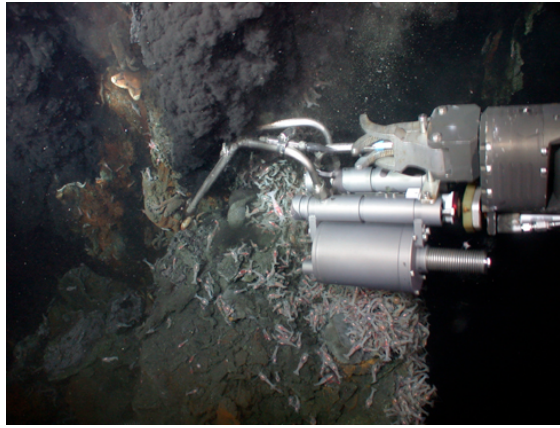


Figure 11. Major pair during exit fluid sampling on Dive 1 (108).

## 8. Water Column Plume Surveys

(Sacha Wichers)

### ***8.1 Velocity measurements***

During the first leg of the STAG experiment we collected CTD data in the neutrally buoyant part of the plume. Sixteen months later we are back at the same site, prepared to take more data. The goal of the plume mapping effort is to identify sensors and methods to find hydrothermal activity autonomously once a CTD cast or a bathymetric map indicates that there is hydrothermal activity in the area. One first order consideration is the ambient currents. Neutrally buoyant plume water at TAG is sheared off and advected down the axial valley on the MAR. We therefore deployed an ADCP on an acoustic release to sample the ambient velocity (Figure 12). We deployed the elevator on October 31<sup>st</sup> around 17:00 GMT at 26° 8.928' N 44° 50.611' W. The ADCP uses a frequency of 300 kHz, and in low bandwidth mode has a range of about 180 meters. We average 4 waterpings per ensemble as we only have 256Mb available on the memory card. The ADCP is set up to ping automatically as fast as possible, with a binsize of 8 meters. This will give a standard deviation of less than 2 cm/s – about equal to the unresolvable bias of the ADCP. The first target of Jason was the elevator so that we could get a visual on it. The elevator is balanced precariously on two legs on a steep slope.

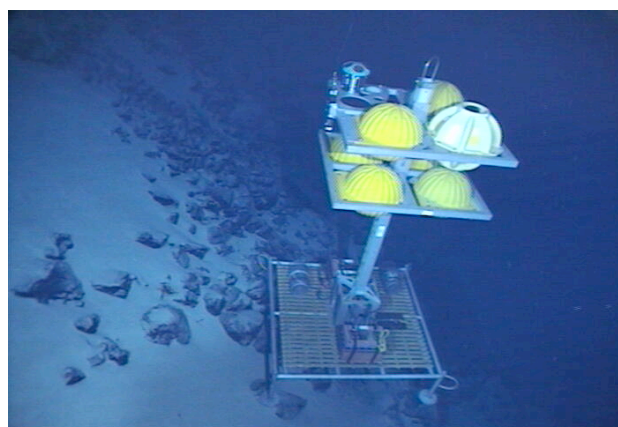
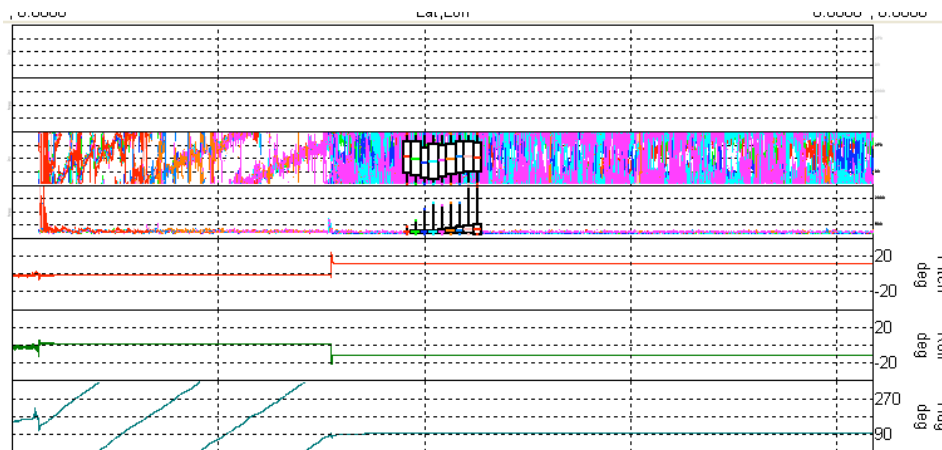


Figure 12. Elevator with ADCP

The ADCP is visible on the rear left corner of the elevator in Figure 11. There are two 24 V batteries in series strapped to the base, as well as two crab traps. The position of the elevator in our XY coordinate frame is  $X=1627$ ,  $Y=4988$ , depth = 3717m. Jason aligned itself with the ‘bow’ of the ADCP and read a heading of around  $90^\circ$ . A first cut at the data shows some intriguing results. Figure 13 shows the first 4 hours of the deployment in RDI’s graphical interface (WinADCP.)



**Figure 13. ADCP data from elevator displayed in WinADCP**

The elevator rotated on its way down, and was both pitched and rolled about 18 degrees upon landing. The heading was indeed 90 degrees as we ascertained with Jason. The first two subplots in Figure 13 give the direction and the magnitude of the velocity, respectively. These two panels are presented in a larger format in Figures 14-15. It is interesting that the elevator was able to profile at greater ranges during ascent and descent. There is one more instance of increased range around ensemble 38000 – perhaps a cloud of scatterers drifted by the elevator. The magnitude of the velocity is nowhere greater than .2 m/s. Further refinement of the data is necessary to give a better value of the average velocity.

We attempted to make velocity measurements in the buoyant stem, but the MAVs’ connector was fouled and the instrument did not work. We also had a 300 kHz ADCP on the vehicle, but we lost communications with the sensor just before attempting to measure vertical velocities in the buoyant part of the plume.

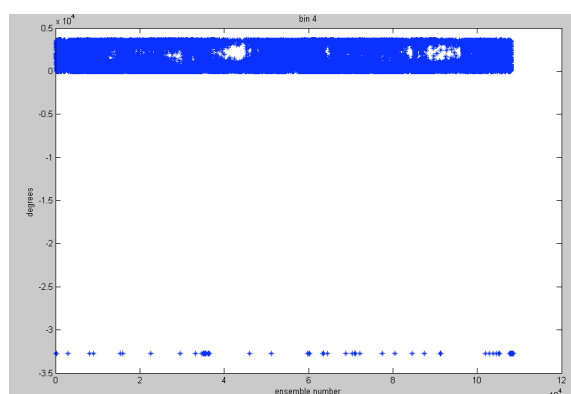


**Figure 14. Velocity direction \* 10.**

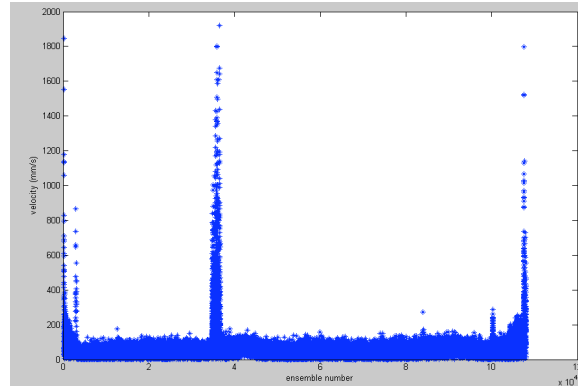


**Figure 15. Velocity magnitude.**

## **8.2 Neutral plume survey**

A Seabird Fastcat 49 CTD and a Webb Labs BBRTD optical backscatter sensor (660 nm wavelength) were mounted to the ROV to measure the lateral extent of the neutrally buoyant plume layer along and across the TAG segment. A background profile of the study area outside the plume was acquired during initial descent on Dive 1 (108) at the elevator site (Figure 16). Note that both temperature and salinity in the North Atlantic decrease with depth.

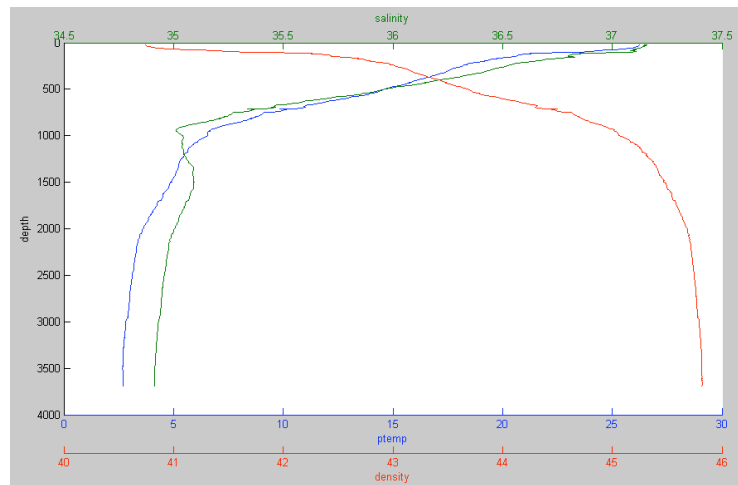


**Figure 16. Background CTD profile.**

The JasonII ROV was towed at a forward speed of about .5 knots on tracklines both along and across the axial valley. Starting from immediately above the TAG mound, the vehicle was towed in a “tow-yo” pattern between ~3000-3500 m depth along a constant heading until the edge of the neutral plume was reached. These tow-yos were conducted at 4 headings corresponding to each of the ridge parallel and ridge normal compass directions. Tow-yo tracklines are shown in Figure 17.

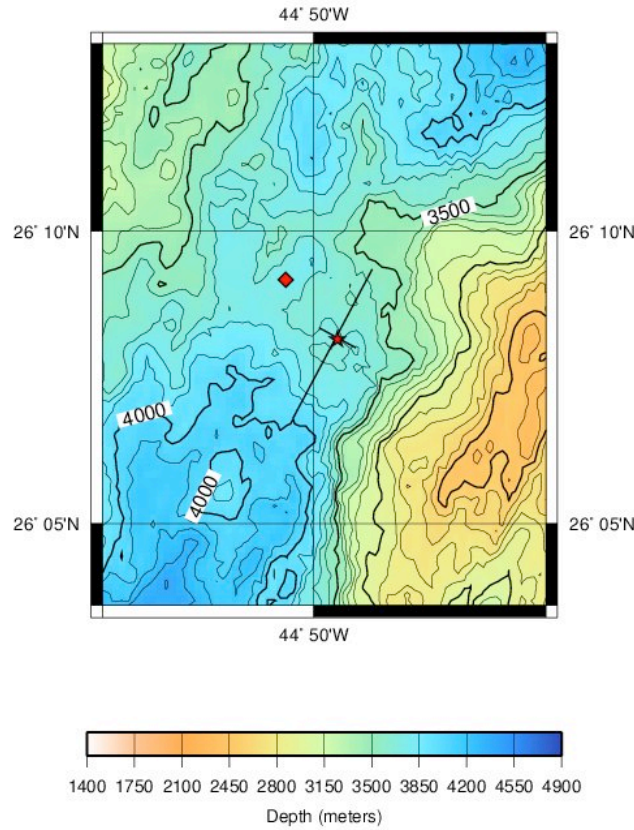


**Figure 17. Tow-yo tracklines. Red square in center of valley is elevator deployment site. Red star in center of cross is TAG mound. Cross lines delineate limit of plumes in tow-yo data.**

The cross in the intersection of the two tracklines is the site of the mound, and the cross in the middle of the axial valley indicates the elevator site. We started the survey on the mound in a south, south westerly direction. We reached the southern limit of the plume ~2.7 km from the mound, then towed the reciprocal course, reaching the plume edge ~2.0 km north of the mound. We returned to the mound, and then towed cross-axis lines, reaching the mound ~0.5 km on either side. An example of CTD data from the neutrally buoyant plume slightly to the northeast of the TAG mound is shown in Figure 18.

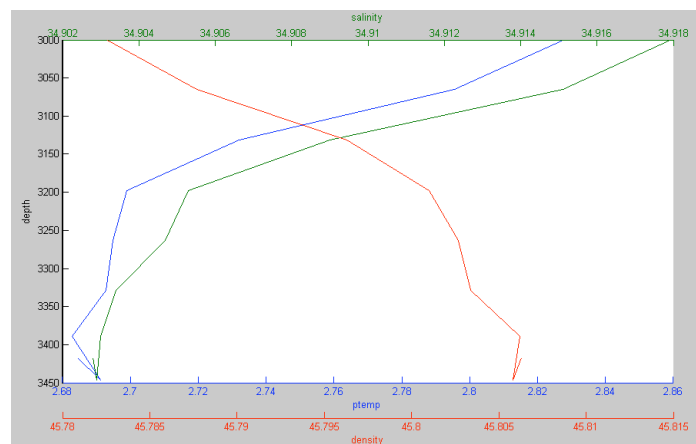


**Figure 18. CTD data from the neutrally buoyant plume.**



The background turbidity at the TAG segment is around 50 counts. In the neutrally buoyant part of the plume the turbidity increases dramatically (Figure 19). Post processing will reveal the correlation between the turbidity of the water as seen by the OBS and the temperature anomaly of the same water mass, and will allow for precise delineation of the plume feature.

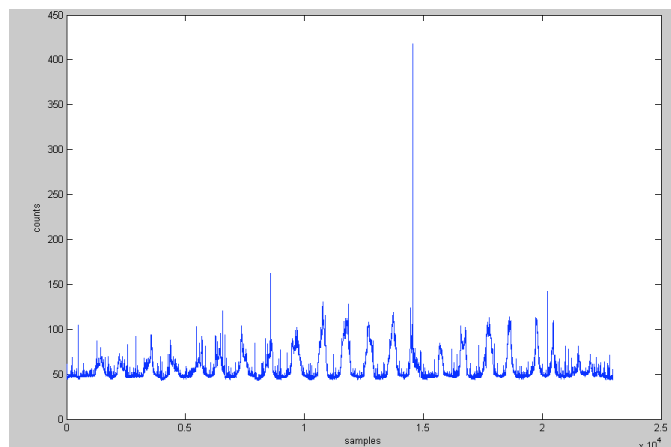


**Figure 19. Optical backscatter measurements during a tow-yo.**

## 9. SM 2000 Microbathymetry Survey

(Chris Roman)

The SM2000 sonar mounted to JASON was used for 4 independent bathymetry surveys and one test of acoustic plume imaging. The sonar was operated from the JASON control van using a new topside computer purchased in October 2004. This was the first field use of the MS2000 (yes MS) topside software. Raw sonar data in .*smb* format was collected to allow post processing of the sonar images. Beam forming and range detection are done in post processing. Profile data as exported by the MS2000 topside software was not recorded because of the inaccuracy of the real time profiling. The real time profiling often selects false bottoms.

<i>Name</i>	<i>Start time (GMT)</i>	<i>End time(GMT)</i>	<i>Purpose</i>
Survey 1	2320 11/01/2004	1030 11/02/2004	Map of TAG mound proper
Survey 2	1934 11/04/2004	2356 11/04/2004	Extend high resolution map to the east
Up wall run	0243 11/04/2004	1000 11/04/2004	Slope contours taken up the east wall
Down wall run	1056 11/04/2004	1737 11/04/2004	Slope contours taken down the wall
Plume imaging	1729 11/02/2004	1735 11/02/2004	Test acoustic plume imaging

**Table 6. Microbathymetry survey information.**

### 9.1 Surveys 1 & 2

Two surveys over the mound were completed to provide higher resolution bathymetry than the current DSL-120 map. These surveys were flown with vehicle altitudes between 15 and 20 meters using the auto-altitude capability of the JASON

control system. The 1200 kHz doppler was used for DVLNAV and was able to maintain bottom lock up to 25 meters of altitude. The nominal forward speed for the vehicle was .5 knots. The speed varied somewhat based on ship motion and the need to keep JASON under Medea. The tracklines were spaced between 15 and 30 meters apart. Tighter tracklines were flown over the mound to ensure overlap with adjacent lines in the high relief areas. North-South and East-West tracklines were flown in the vicinity of the TAG vent to remove occlusions caused by the relief and provide better coverage of the vent area. Although the SM2000 sonar raw data can be beam formed to a 120 degree swath angle, a 90 degree swath angle was assumed to conservatively plan the track line spacing. The sonar was run at a ping rate of 1 Hz, which correlates to a sub beamwidth forward motion of the vehicle at a nominal speed of .5 knots.

Post processing the survey data includes beam forming, range detection, sensor offset calibrations and re-navigation of the LBL and doppler bottom lock position estimates. The heading source for the re-navigation is the OCTANS fiber optic gyro. Initial processed bathymetry swaths indicate that the resulting map could be gridded down to .5 meter resolution.

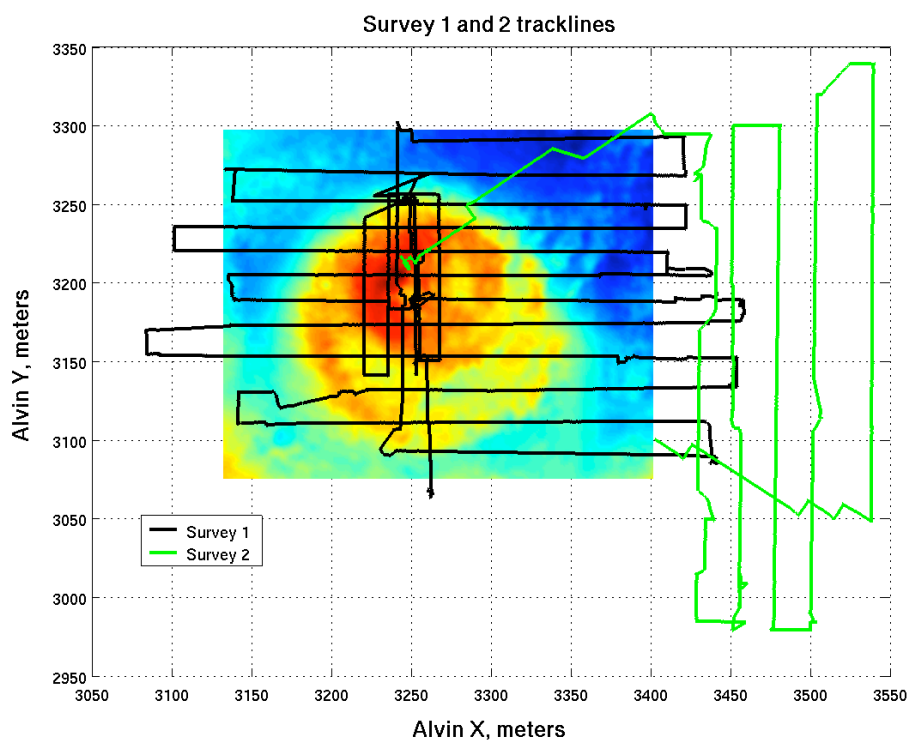


**Figure 20. Tracklines of surveys 1 & 2 superimposed on pre-existing DSL-120 bathymetry.**



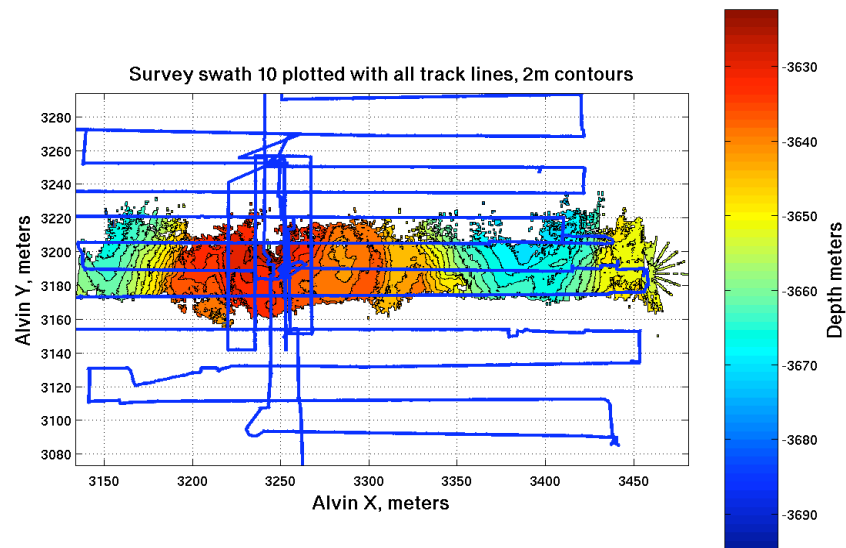


Figure 21. Swath data from line 10 with all tracklines.

## 9.2 Wall runs

The SM2000 was run during the transects up and down the eastern wall. These survey lines should provide meter scale or better shape information over the swath width. The up slope transect was flown at low altitude (< 6 meters) so visual observations could be made. The down slope transect was flown between 20 and 25 meters of altitude and has a greater swath width. These surveys were also completed at a nominal speed of .5 knots. The sonar was run at 1 Hz and all of the raw data was recorded.

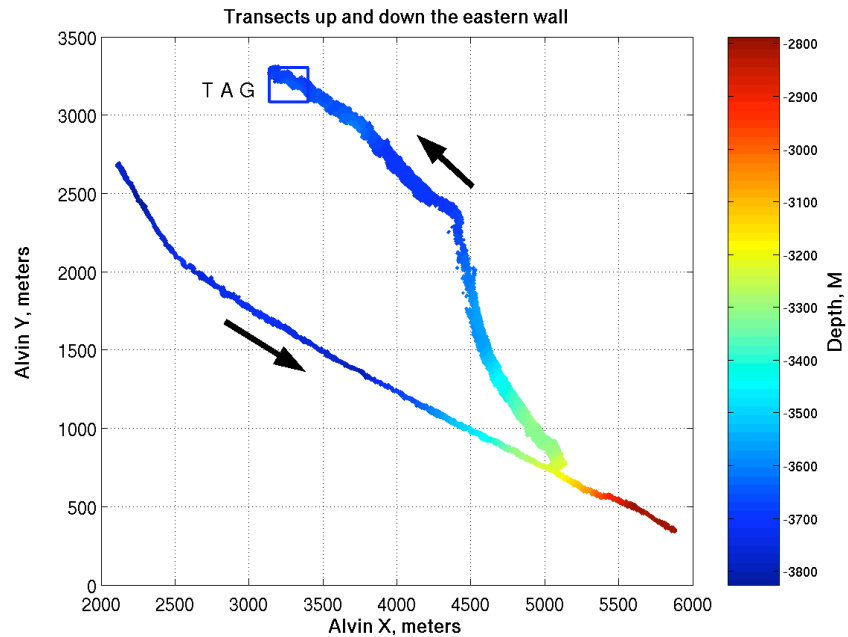
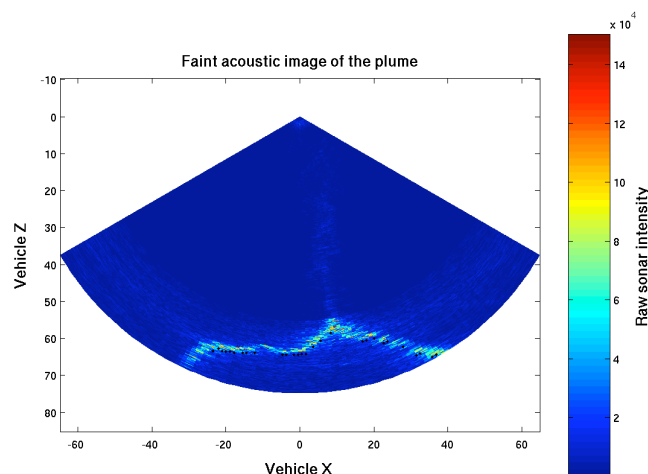


Figure 22. Preliminary bathymetry from east wall transects.

### 9.3 Plume Detecting

The SM2000 was used to investigate how far off the sea floor the plume could be imaged acoustically. The test was performed by JASON moving laterally into the plume from clear water and then moving in 10 meter depth increments higher in the water column while remaining in the plume stem. The sonar gains were continuously adjusted to maintain an image of the plume. The plume was clearly detectable at low altitudes, 10 m off of the bottom, and the acoustic signature faded between 80 and 100 meters off the bottom. Although the plume is visible at low altitudes it did not affect bottom detection and mapping with the sonar.



**Figure 23.** The TAG plume is visible in this sonar image rising from the peak in the seafloor.

## 10. Green Laser Testing

(Clifford Pontbriant)

Hydrothermal plume measurements are presently made via point source measurements of thermal, particulate, or chemical parameters. Thus it is necessary to pass the sensors directly through a plume to detect it. Clearly the search for hydrothermal plumes and thus deep-sea vent fields would be facilitated if plumes could be detected from a distance. Al Bradley and Rob Reves-Sohn are PIs on a WHOI funded project to develop a green laser system capable of detecting optical anomalies in hydrothermal plumes from a distance. Clifford Pontbriant is the primary lab technician for the project, and he took part in the dive program to perform initial testing of the prototype green laser source system. The instrument design consists of a pair of green lasers and an optical detector and scanning telescope. Each laser is mounted so the beam projects perpendicular to the vehicle, one to port, the other to starboard. The telescope and detector are mounted approximately one meter away from the lasers, and the telescope scans along the laser beams, looking for optical backscatter. The scanning telescope returns its orientation, so each backscatter signal will be assigned a position along the beam. This design offers an improved range over the point-source optical backscatter detector currently used in hydrothermal plume detection, particularly in finding the relatively narrow plume stem.

Determining the extent of this improvement was a primary goal of the TAG trials.

In order to test the concept rigorously and to take advantage of Jason's high bandwidth, the trial design incorporated a high sensitivity wide-angle camera as the light detector. The camera eliminated the need for a scanning telescope, and was sensitive enough for the job. The video feed from the camera was recorded and displayed in the Jason control van. Not only did the camera pose as a suitable detector, it gave instantaneous qualitative results that helped guide the survey process.

The top panel of Figure 24 is a plot of signal strength and angle from the vehicle ( $90^\circ$  is normal to the vehicle, parallel to the beam) for thirty seconds of video from the first dive. This plot is analogous to the instrument's raw data. The bottom panel of Figure 24 is a plot from the same thirty seconds of video, but plotted against distance from the vehicle rather than angle. The backscatter signal is centered around 2.3 meters from the vehicle, off the starboard side. There is a faint signal 4.25 meters out at 20 to 25 seconds, but it is hard to pick up in this plot. Notice how the density of data points increases inversely with distance; a product of the geometries of the system.

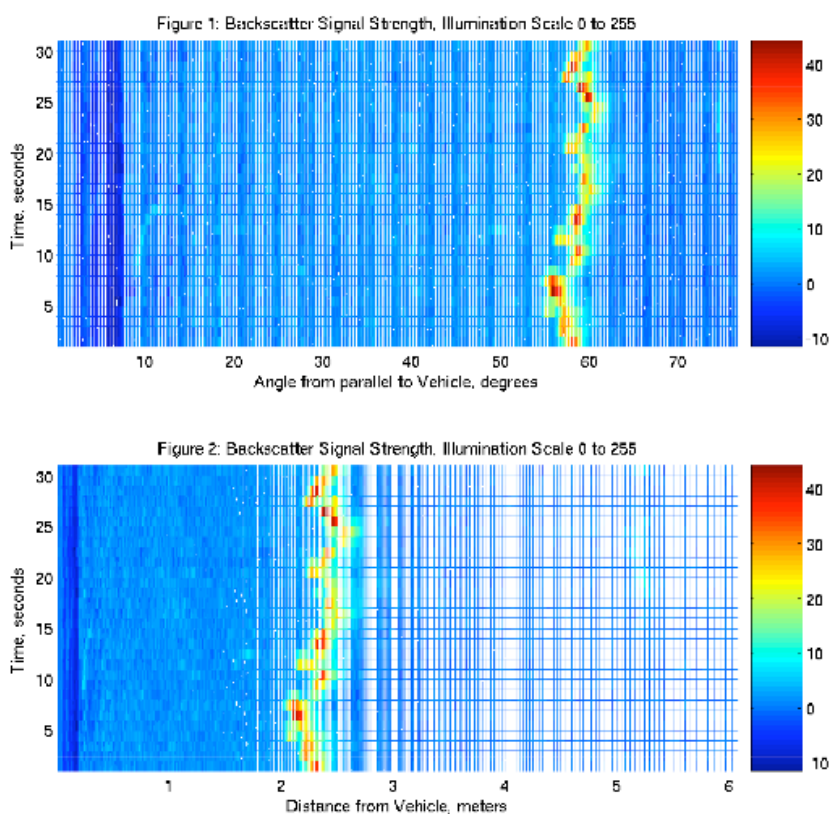


**Figure 24. Green laser backscatter strength as a function of distance from the vehicle and time of flight.**

Backscatter was observed from within two meters of the vehicle to beyond ten meters. The first trials came on the back of temperature probe recovery on the ocean bottom during the first dive. Backscatter was observed from terrain features, particles stirred by the vehicle, and, most importantly, black smokers. The second trials came during the second dive, and incorporated surveys of the buoyant plume stem fifty meters above the bottom. Strong backscatter was encountered in this region, which is very promising, since the usefulness of this instrument as a vent finding tool is its ability to detect the long, narrow plume stem.

## Appendix A – Cruise Participants

Name	Position	Institution	email
Rob Reves-Sohn	Chief scientist	WHOI	rsohn@whoi.edu
Susan Humphris	Co-chief	WHOI	shumphris@whoi.edu
Chris Roman	GRA	WHOI	croman@whoi.edu
Ella Atkins	Scientist	U. Maryland	ella@ssl.umd.edu
Rhian Waller	Scientist	WHOI	rwaller@whoi.edu
Clifford Pontbriand	Laser tech	WHOI	Clifford.pontbriand.03@mckenna.edu
Cathy Offinger	DSG	WHOI	coffinger@whoi.edu
Sacha Wichers	GRA	WHOI	wichers@mit.edu
Andy Bowen	DSG	WHOI	abowen@whoi.edu
Will Sellers	DSG/Exp. Leader	WHOI	wsellers@whoi.edu
Jim Varnum	DSG	WHOI	jimv@drizzle.com
Peter Collins	DSG	WHOI	pcollins@whoi.edu
Bob Waters	DSG	WHOI	rwaters@whoi.edu
Chris Taylor	DSG	WHOI	ctaylor@whoi.edu
Will Handley	DSG	WHOI	handleys@compuserve.com
Brian Bingham	DSG	WHOI	bbingham@whoi.edu
Tom Crook	DSG	WHOI	tcrook@whoi.edu
Steve Gegg	DSG	WHOI	sgegg@whoi.edu
Darryl Green	Scientist	SOC	drhg@soc.soton.ac.uk
Jon Copley	Scientist	SOC	jtc@mercury.soc.soton.ac.uk
Belinda Alker	Fluids tech	SOC	b.alker@soc.soton.ac.uk
Sarah Bennett	GRA	SOC	saroban@soc.soton.ac.uk
Caroline Peacock	GRA	U. Bristol	Caroline.Peacock@bristol.ac.uk
Carla Sands	GRA	SOC	cms600@soc.soton.ac.uk
Hannah Flint	GRA	SOC	hcf1@soc.soton.ac.uk
Magdalena Szuman	Research tech	SOC	msz@soc.soton.ac.uk

## ***Appendix B. Digital Images of Temperature Probes***



**Figure B1. High-temperature probe #2, marker #4.**



**Figure B2. High-temperature probe #3, marker 12.**

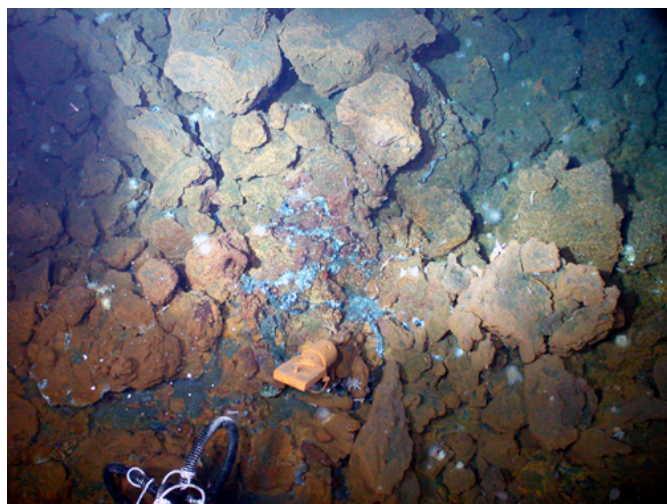


**Figure B3. High-temperature probe #4.**





**Figure B4. High-temperature probe #5.**



**Figure B5. High-temperature probe #6.**

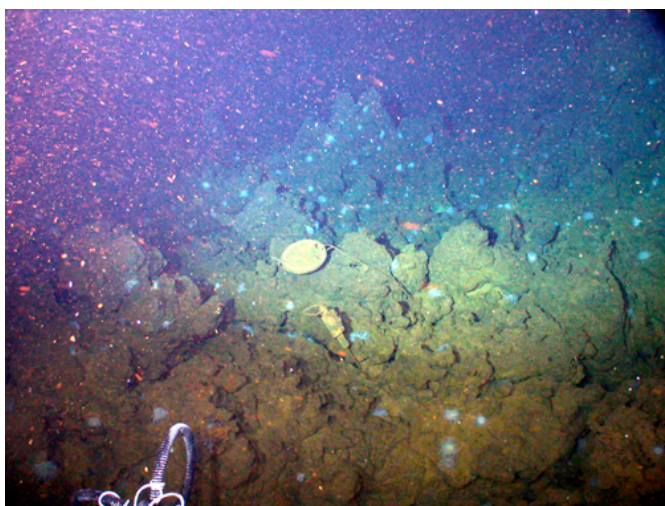


**Figure B6. Intermediate-temperature probe #13, marker #10.**

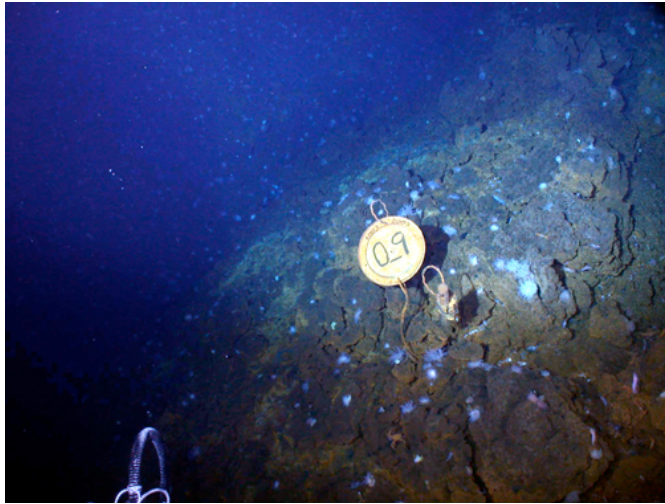


**Figure B7. Intermediate-temperature probe #14, marker #9.**

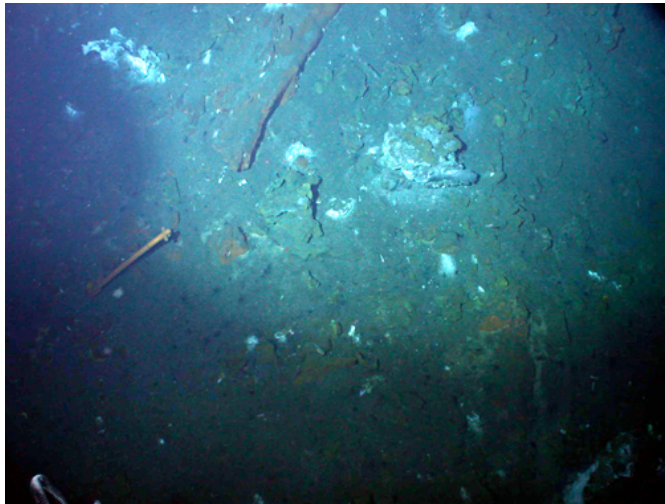


**Figure B8. Low-temperature probe #1.**

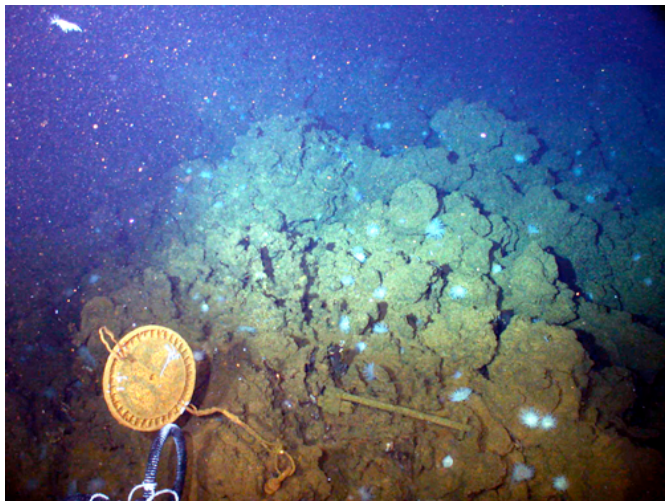


**Figure B9. Low-temperature probe #2, marker #5.**



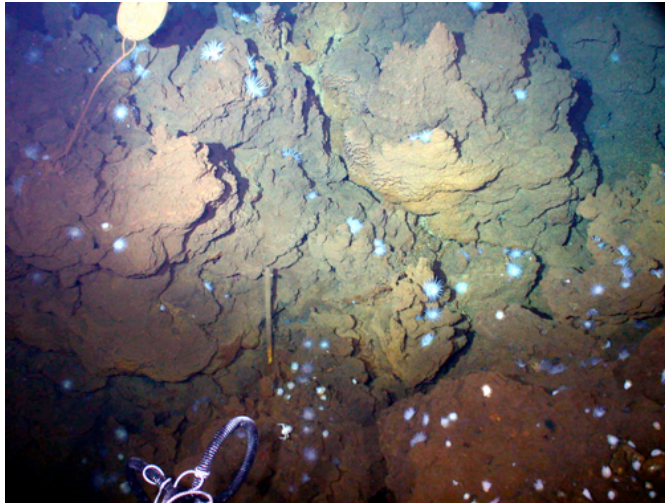


**Figure B10. Low-temperature probe #3 (burned, no data), marker #6.**



**Figure B11. Low-temperature probe #4, marker #4.**

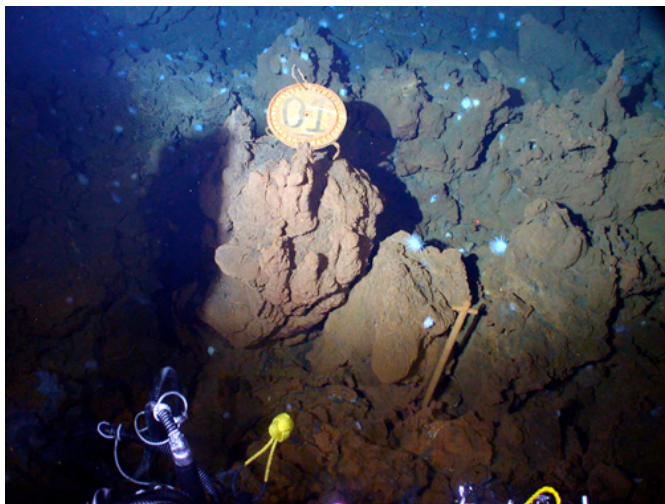


**Figure B12. Low-temperature probe #5, marker #1.**



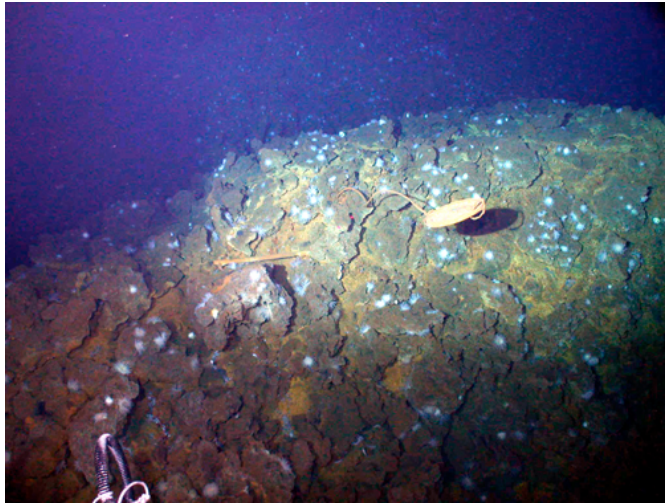


**Figure B13. Low-temperature probe #6, marker #3.**

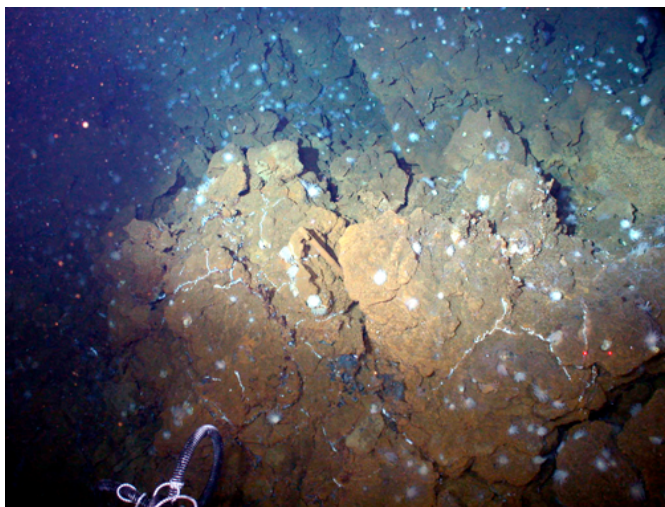


**Figure B14. Low-temperature probe #7, marker #13.**



**Figure B15. Low-temperature probe #8, marker #2.**

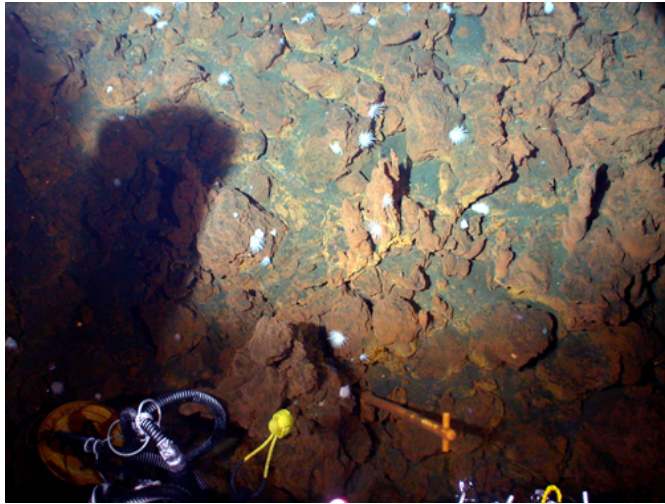


**Figure B16. Low-temperature probe #9.**

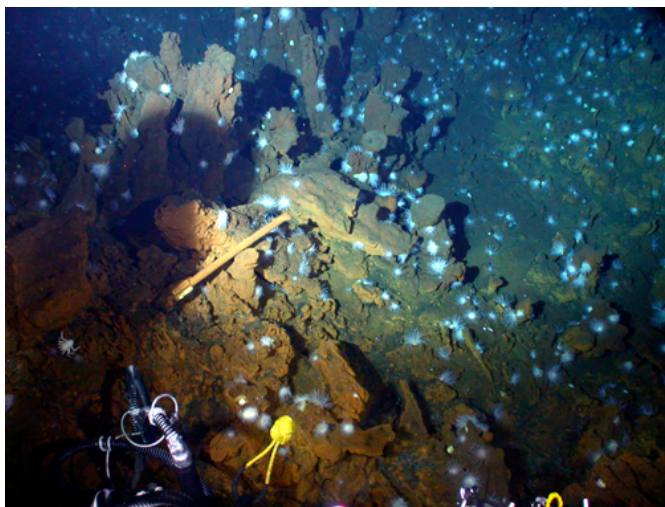


**Figure B17. Low-temperature probe #10 (burned, no data).**

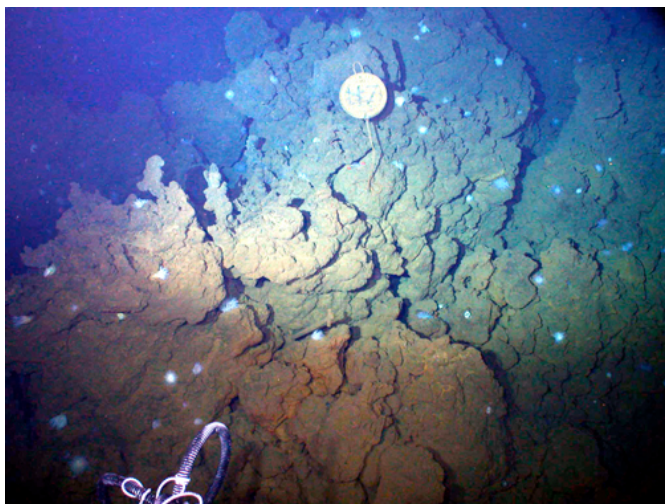


**Figure B18. Low-temperature probe #11, marker #H7.**

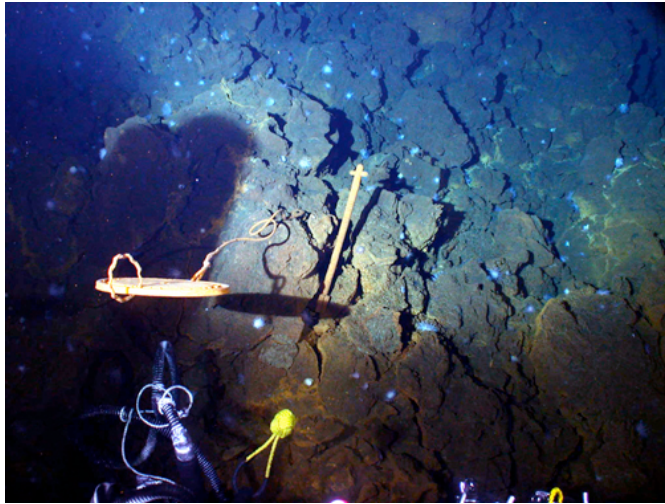


**Figure B19. Low-temperature probe #12, marker #8.**

## Appendix C. Station Table

### KNORR 180-1: Jason2 SAMPLING STATIONS

Station #	Date	Time (Z)	Location		Depth (m)	Location Description	Sample type
			°N	°W			
<b>Lowering: Jason2-108</b>							
J2-108-1	11/1/04	22:56	26°08.231'	44°49.559'	3623	Top of BSC	2 crab traps
J2-108-2	11/2/04	11:32	26°08.156'	44°49.555'	3655	Off S. edge of lower platform	Oxidized sulfide
J2-108-3	11/2/04	12:31	26°08.184'	44°49.551'	3641	S. part of lower platform	Oxidized sulfide
J2-108-4	11/2/04	12:55	26°08.201'	44°49.549'	3635	S. edge of upper platform	Massive sulfide
J2-108-5	11/2/04	13:41	26°08.218'	44°49.549'	3632	Mid-upper platform, near ODP cone	Massive sulfide
J2-108-6	11/2/04	15:11	26°08.198'	44°49.558'	3625	Top of BSC; near crab traps	Shrimp slurp sample
J2-108-7	11/2/04	15:33	26°08.145'	44°49.558'	3625	Top of BSC; near crab traps	Shrimp slurp sample
J2-108-8	11/2/04	16:27	26°08.142'	44°49.560'	3621	Top of BSC	Hi-T fluid sample
<b>Lowering: Jason2-109</b>							
J2-109-1	11/3/04	04:49	26°08.233'	44°49.555'	3628	Slope of BSC	2 crab traps
J2-109-2	11/4/04	10:47	26°06.795'	44°48.357'	3082	First fault, E. wall median valley	Gabbro
J2-109-3	11/4/04	17:39	26°08.312'	44°49.689'	3665	NW of TAG mound	2 push cores
J2-109-4	11/4/04	18:31	26°08.321'	44°49.748'	3655	Tide gauge location	Background fluid sample
J2-109-5	11/5/04	00:29	26°08.237'	44°49.561'	3633	NW slope of TAG mound	Push core
J2-109-6	11/5/04	01:31	26°08.219'	44°49.590'	3634	W. part of lower platform	Push core
J2-109-7	11/5/04	02:45	26°08.234'	44°49.557'	3630	Slope of BSC; near crab traps	Shrimp slurp sample
J2-109-8	11/5/04	02:50	26°08.233'	44°49.556'	3629	Slope of BSC; near crab traps	Shrimp slurp sample
J2-109-9	11/5/04	03:20	26°08.230'	44°49.559'	3620	Top of BSC	Crab grab
J2-109-10	11/5/04	04:41	26°08.231'	44°49.559'	3625	Top of BSC	Hi-T fluid sample; chimney



## Appendix D. Biological Specimen Lists

Table D1 - Specimens Collected for Molecular Work

Dive	Date	Location	Depth	Species	No.	-70	EtOH
Elevator	02-Nov-04	Elevator crab trap	3703	Amphipod - <i>Eurythenes gryllus</i>	1		1
Elevator	02-Nov-04	Elevator crab trap	3703	Amphipods - Large	1		1
Elevator	02-Nov-04	Elevator crab trap	3703	Amphipods - light orange large	36	30	6
Elevator	02-Nov-04	Elevator crab trap	3703	Amphipods - orange small	26	20	6
Elevator	02-Nov-04	Elevator crab trap	3703	Amphipods - Red	3		3
Elevator	02-Nov-04	Elevator crab trap	3703	Amphipods - White	106	100	6
J2-108	02-Nov-04	St#1	3623	<i>Rimicaris exoculata</i> - ADULT	15	15	
J2-108	02-Nov-04	St#2		Sulphide Sample	pieces	y	
J2-108	02-Nov-04	St#3		Sulphide Sample	pieces	y	
J2-108	02-Nov-04	St#4		Sulphide Sample	pieces	y	
J2-108	02-Nov-04	St#6	3625	<i>Rimicaris exoculata</i> - Adolescent	13	13	
J2-108	02-Nov-04	St#6	3625	<i>Rimicaris exoculata</i> - Adult	4	4	
J2-108	02-Nov-04	St#6	3625	<i>Rimicaris exoculata</i> - Juvenile	206	206	
J2-108	02-Nov-04	St#7	3625	<i>Rimicaris exoculata</i> - Adolescent	6	6	
J2-108	02-Nov-04	St#7	3625	<i>Rimicaris exoculata</i> - Juvenile	36	36	
J2-109	04-Nov-04	St#1	3628	Chorocaris	7	7	
J2-109	04-Nov-04	St#1	3628	<i>Rimicaris exoculata</i> - Juvenile	271	271	
J2-109	04-Nov-04	St#1	3628	<i>Rimicaris exoculata</i> - Adolescent	9	9	
J2-109	04-Nov-04	St#1	3628	<i>Rimicaris exoculata</i> - Adult	46	46	
J2-109	04-Nov-04	St#7	3629	<i>Rimicaris exoculata</i> - Juvenile	137	137	
J2-109	04-Nov-04	St#7	3629	<i>Rimicaris exoculata</i> - Parasitic	3		3
J2-109	04-Nov-04	St#7	3629	<i>Rimicaris exoculata</i> - Adult	4	4	
J2-109	04-Nov-04	St#8	3629	<i>Rimicaris exoculata</i> - Juvenile	14	14	

Table D2 - Specimens Collected for Epibiont Work

Dive	Date	Location	Depth	Species	No.	-70	EtOH
J2-108	02-Nov-04	St#6	3625	<i>Rimicaris exoculata</i> - Juvenile	50	50	
J2-109	04-Nov-04	St#1	3628	<i>Rimicaris exoculata</i>	20	20	
J2-109	04-Nov-04	St#1	3628	<i>Chorocaris chacei</i>	2	2	
J2-109	04-Nov-04	St#9	3620	Crabs	3	3	

**Table D3 - Reproductive histology & TMAO shrimp sample summary**

<b>Dive</b>	<b>Sample station #</b>	<b>Sample</b>
Jason 108	1 (crab trap)	15 adult <i>R. exoculata</i> thoraxes fixed for histology
	6 (1 <sup>st</sup> slurp sample)	4 adult + 14 "adolescent" <i>R. exoculata</i> thoraxes fixed for histology 161 juvenile <i>R. exoculata</i> frozen whole for TMAO
	7 (2 <sup>nd</sup> slurp sample)	6 "adolescent" <i>R. exoculata</i> thoraxes fixed for histology
Jason 109	1 (crab trap 1)	38 adult + 8 "adolescent" <i>R. exoculata</i> thoraxes fixed for histology 35 "adolescent" <i>R. exoculata</i> frozen whole for TMAO 2 adult <i>C. chacei</i> thoraxes fixed for histology 2 adult <i>C. chacei</i> abdominal muscle samples frozen for TMAO
	1 (crab trap 2)	9 adult <i>R. exoculata</i> thoraxes fixed for histology 3 adult <i>C. chacei</i> thoraxes fixed for histology 3 adult <i>C. chacei</i> abdominal muscle samples frozen for TMAO
	7 (1 <sup>st</sup> slurp sample)	4 adult <i>R. exoculata</i> thoraxes fixed for histology
n/a	Elevator crab traps	10 non-vent amphipods frozen for TMAO

## ***Appendix E. JASON2 Navigation***

*The purpose of the navigation was to provide the following:*

- a) Precise positions of underwater vehicles
- b) Dynamic Positioning of the R/V Knorr from the control van
- c) Display, log, and distribute navigation data

### ***Major Navigation System Components***

- 1) Benthos 455 Acoustic Signal Processor
- 2) Kongsberg/Simrad SDP10/11 Dynamic Positioning System
- 3) C-Nav Dual Frequency Corrected GPS System
- 4) Benthos TR6000 Recoverable Transponders
- 5) Ametek/Straza SP23LT Transducer

### ***Long BaseLine Transponders (LBL)***

LBL transponders were deployed to provide acoustic navigation of MEDEA and JASON. Three transponders were initially deployed at TAG based on available topographical information. Transponders were located to optimize coverage and eliminate shadowing when topography interfered with the acoustics. The transponders were deployed with 200 meter tethers and shorter than normal baseline lengths (~2800M) to improve coverage of the TAG mound.

### ***Surveying the transponders***

Accurate three dimensional transponder positions are needed to provide a precise location of the underwater vehicles. The transponders were surveyed in using WHOI software written by Dr. Dana Yoerger. The survey software corrects for ship heading, sound velocity, ship movement, and gps-transducer offsets. The problem is a linear least-squares problem, so the answer is exact and unique. Survey data was collected in a circular pattern around each of the 3 transponders at radius of 2 km and a speed of 5 knots. Matlab and GPSCAL4 were used to calculate the positions down to a GA. Sound velocity came from a T-5 XBT (1830m) and the Levitus tables for the deeper velocities.

### ***Navigation during JASON II dives***

Navigation consisted of controlling the ship dynamic positioning system to follow a predetermined track line at a consistent speed while receiving acoustic positions of JII and MEDEA or moving to a specific location. The preferred LBL method is to receive the transponder replies at the vehicles and then up the fiber optic link to the acoustic processor. LBL fixes were used to update Jason doppler navigation in the DVL system.

### ***Navigation during SM2000 micro bathymetry survey***

The objective was to have JASON II follow predetermined track lines at .5 knots. Jason doppler position was updated with Jason LBL fix as necessary

### *Navigation during JASON survey*

Transponders were deployed with 200meter tethers to facilitate Jason maneuvering around topography near the bottom. The Knorr was positioned with DP to hold Media over the desired survey area allowing Jason to safely run around on its tether. Ship, Medea, and Jason were navigated and positions displayed at all times. There were few holes in the acoustic coverage of the TAG mound.

### *Elevator with 300Khz ADCP Acoustic Doppler Current Profiler*

The elevator was deployed from the surface about 2km NW of Tag. Once on the bottom the elevator was shadowed from all transponders. Bottom location was determined by surveying the elevator as we do transponders. The location from the survey proved to be DNO. Recovery of the elevator was uneventful.

### *Overall*

Acoustic navigation and dynamic positioning performed well allowing for efficient use of ship time. Repeatability and locating specific features was excellent. The navigation was crucial to the mapping and aided in the resolution of ambiguities. All transponders were recovered. Tether wire was 1/16 inch aircraft cable which sank to bottom after transponder release.